

Magnetically ordered Kondo lattice in YbNi_2Ge_2 at high pressure

This article has been downloaded from IOPscience. Please scroll down to see the full text article.

2001 J. Phys.: Condens. Matter 13 10935

(<http://iopscience.iop.org/0953-8984/13/48/318>)

View [the table of contents for this issue](#), or go to the [journal homepage](#) for more

Download details:

IP Address: 171.66.16.238

The article was downloaded on 17/05/2010 at 04:37

Please note that [terms and conditions apply](#).

Magnetically ordered Kondo lattice in YbNi₂Ge₂ at high pressure

G Knebel¹, D Braithwaite¹, G Lapertot¹, P C Canfield² and J Flouquet¹

¹ Département de Recherche Fondamentale sur la Matière Condensée, SPSMS, CEA Grenoble, 38054 Grenoble, France

² Department of Physics and Astronomy and Ames Laboratory, Iowa State University, Ames Iowa, IA 50011, USA

E-mail: knebel@drfmc.ceng.cea.fr

Received 22 August 2001

Published 16 November 2001

Online at stacks.iop.org/JPhysCM/13/10935

Abstract

We have studied the electrical resistivity of YbNi₂Ge₂ under hydrostatic pressure up to 100 kbar. With increasing pressure the system is continuously tuned from an intermediate valence state at low pressure to a magnetically ordered Kondo lattice at high pressure. The critical pressure for the appearance of a magnetic ground state is near 50 kbar. Below P_c the resistivity shows a T^2 dependence, characteristic of a Fermi liquid description at low temperatures. The coefficient of the T^2 term increases drastically on approaching P_c . Above P_c , the magnetic transition temperature T_m increases linearly with pressure. The magnetoresistance at high pressure suggests the importance of ferromagnetic coupling.

1. Introduction

In Kondo lattice compounds the ground-state properties are crucially determined by the competition of the RKKY interaction and the Kondo interaction. The energy scales of both interactions are related to the effective hybridization strength $N(E_F)J$ between the 4f and conduction electrons, $T_{\text{RKKY}} \propto (N(E_F)J)^2$ and $T_K \propto \exp(-1/N(E_F)J)$ [1, 2]. Here J is the coupling constant between the localized f moments and the conduction electrons and $N(E_F)$ is the density of states at the Fermi level. For large J the Kondo interaction dominates the RKKY interaction and leads to a screening of the 4f moments. The most interesting case occurs in the heavy fermion systems where the energy scales of the two interactions are almost of the same order of magnitude, which makes these systems very close to a magnetic instability. By applying an external or chemical pressure P it is possible to purposely change the hybridization strength and to tune these systems through a magnetic quantum critical point (QCP).

For Ce Kondo lattice compounds increasing pressure leads to an increase of the hybridization strength and favours a non-magnetic ground state Ce⁴⁺ (4f⁰) over the magnetic Ce³⁺ (4f¹)

state. The transition from magnetic order to a non-magnetic state has been extensively studied for many systems, e.g. CeCu₂Ge₂ [3], CePd₂Si₂ [4], CeRh₂Si₂ [5] or CeIn₃ [6]. Here, the pressure-induced transition from the antiferromagnetically ordered to the paramagnetic state is well described by the spin fluctuation theory for a QCP [7–9]. At the critical pressure, where $T_N \rightarrow 0$, one observes strong deviations from Landau Fermi liquid behaviour due to the low energy and extended spin fluctuations. At very low temperatures these systems show a superconducting transition with a possibly magnetically mediated pairing mechanism [10].

The electron–hole analogy between the Yb³⁺ (4f¹³) and the Ce³⁺ (4f¹) electronic configuration offers the possibility to go the other way round and to induce a magnetically ordered phase due to the application of pressure. Increasing pressure favours the trivalent magnetic Yb³⁺ (4f¹³) over the divalent non-magnetic Yb²⁺ (4f¹⁴) state due to the reduction of the unit cell volume. Thus the energy difference between the 4f level and the Fermi level increases and valence fluctuations are suppressed, and a decrease of the effective hybridization strength $|JN(E_F)|$ is expected. In contrast to the Ce Kondo lattice compounds there only exist a few examples of Yb Kondo lattice compounds with Kondo (or spin fluctuation) temperatures in the range $10 < T_K < 100$ K, corresponding to systems which are near a magnetic instability. Pressure-induced magnetic transitions have been observed in the initially at $P = 0$ non-magnetic compounds YbCuAl [11], Yb₂Ni₂Al [12] and YbCu₂Si₂ [13, 14]. In the system YbCu_{5-x}Al_x an antiferromagnetically ordered ground state is found for Al concentrations $x > 1.5$ [15]. As in the Ce compounds one finds non-Fermi liquid effects at the border to the magnetic order. Recent studies on the antiferromagnetically ordered compound YbRh₂Si₂ with a very low ordering temperature $T_N = 0.065$ K have encouraged intensive studies on the QCP in Yb compounds [16].

In this paper we study the temperature–pressure phase diagram of the paramagnetic compound YbNi₂Ge₂. At ambient pressure the enhanced Sommerfeld coefficient of the specific heat $\gamma = 136$ mJ mol⁻¹ K⁻² suggests a strong 4f-conduction electron hybridization [17]. In comparison to the expected value $\mu = 4.54\mu_B$ for the free magnetic moment of the Yb³⁺ state the effective magnetic moment shows only a value of $\mu_{\text{eff}} = 3.51\mu_B$, which is possibly caused by an intermediate valence state of Yb. The magnetic susceptibility at ambient pressure is anisotropic with $\chi_{ab} > \chi_c$ and follows a Curie–Weiss behaviour $\chi = C/(T + \theta)$ above 100 K. The sign of the paramagnetic Curie temperature depends on the orientation, $\theta_c = -47.5$ K and $\theta_{ab} = 18.5$ K: for the average this yields $\theta_{\text{ave}} = 2$ K [17]. However, this anisotropy is much less than in YbRh₂Si₂, where $\chi_{ab} \approx 100\chi_c$. The strong anisotropy in real space may be a hint to a quasi-two-dimensional magnetic fluctuation spectrum in the reciprocal space [16].

In Ce Kondo lattice compounds it has been shown that the substitution of Ge by Si in ThCr₂Si₂ is mainly a volume effect and can be qualitatively compared with experiments under hydrostatic pressure [18, 19]. The isostructural compound of YbNi₂Ge₂, YbNi₂Si₂, has a smaller unit cell and orders magnetically at $T_N = 2.1$ K [20, 21]. If we regard the unit cell volume of YbNi₂Si₂ as the critical volume for a magnetically ordered state ($V \approx 146$ Å³, which corresponds to the volume of YbCu₂Si₂ at the critical pressure [14]), we expect a critical pressure for YbNi₂Ge₂ of $P \approx 100$ kbar (assuming a Murnaghan equation of state with a bulk modulus $B_0 = 1680$ kbar and $B'_0 = 0.8$ comparable to other Yb compounds [14]), which is experimentally achievable with hydrostatic pressure techniques.

2. Experimental details

Single crystals of YbNi₂Ge₂ were grown out of an In flux. Details of the sample preparation are given in [17]. X-ray powder diffraction patterns confirmed the single-phase samples which crystallize into ThCr₂Si₂ (*I4/mmm*) with lattice parameters $a = 4.001$ Å and $c = 9.733$ Å.

The crystals grow plate-like with the c direction perpendicular to the plates. From these plates small pieces were cleaved and a small sample of $600 \mu\text{m} \times 100 \mu\text{m} \times 65 \mu\text{m}$ was prepared by polishing. The resistivity was measured in the ab plane. The resistivity ratio of the sample is rather low, $\rho(300 \text{ K})/\rho(4.2 \text{ K}) \approx 7.5$, and the residual resistivity at ambient pressure is $\rho_0 = 7.6 \mu\Omega \text{ cm}$. There were no indications of filamentary superconductivity of In.

The high-pressure measurements were performed in a Bridgman type cell with non-magnetic anvils of tungsten carbide and a pyrophyllite gasket. The sample is placed in the middle of the gasket between two discs of steatite which transmit the pressure. The pressure was determined by the superconducting transition of a thin Pb foil which is placed near the sample in the cell. The width of the transition of Pb was 0.03 K at low pressures and 0.1 K at the highest investigated pressure, $P = 96 \text{ kbar}$. This corresponds to maximal pressure gradients of 2 kbar at the highest pressures. The resistivity was measured using a standard four-point lock-in technique at 11.7 Hz. The measuring current was $100 \mu\text{A}$ at the lowest temperatures. It was carefully checked that there were no self-heating effects due to the current. The measurements were performed in a conventional ⁴He cryostat and in a dilution refrigerator down to 40 mK. Here it was possible to measure in magnetic fields up to $H = 8 \text{ T}$ with $H \perp (ab)$.

3. Experimental results

Figure 1 shows the temperature variation of the resistivity at ambient pressure and at $P = 96 \text{ kbar}$. At zero pressure the resistivity decreases monotonously from the room temperature value to low temperatures. Around 100 K there is a very broad shoulder. However, at high pressures (96 kbar) the resistivity shows a very pronounced minimum at 20 K and a maximum at lower temperatures. The resistivity at 300 K decreases continuously under pressure. The upper inset in figure 1 shows the temperature dependence of the magnetic contribution ρ_m to the resistivity, which is determined by subtracting the temperature-dependent contribution

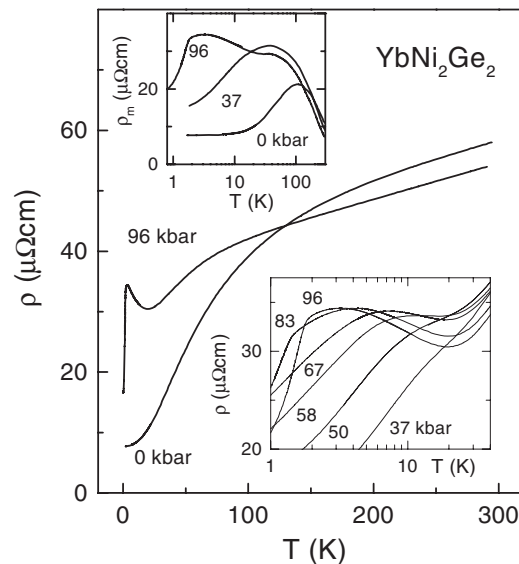


Figure 1. Temperature dependence of the resistivity of YbNi₂Ge₂ for different pressures. The upper inset shows the magnetic contribution to the resistivity. The lower inset shows the evolution of the low-temperature maximum with increasing pressure.

of the resistivity of the isostructural non-magnetic compound LuNi_2Ge_2 [17]. ρ_m shows a very broad, but pronounced, peak at $T_H^{\text{max}} \approx 100$ K which may indicate the incoherent Kondo scattering processes on crystal field levels. Under pressure this maximum shifts to lower temperature, but still stays very broad. At 37 kbar we find $T_H^{\text{max}} \approx 38$ K. However, at higher pressures T_H^{max} is almost constant at $T_H^{\text{max}} \approx 34 \pm 1$ K. As shown in the lower inset in figure 1 at low temperatures a second peak starts to develop for pressures higher than 37 kbar. At 37 kbar there is only a small shoulder to see, but with increasing pressure it becomes more and more pronounced and at 67 kbar we observe a clear minimum and an increase to lower temperatures. This increase in the resistivity is clearly due to the incoherent single-ion Kondo scattering. Below the minimum $\rho(T)$ increases logarithmically at lower temperatures. At low temperatures and high pressure the resistivity decreases again due to the formation of a Kondo lattice state. The low-temperature maximum T_L^{max} is a measure of the Kondo temperature T_K of the low-energy crystal-field doublet of the system at low temperature. In axial symmetry, the $J = 7/2$ 4f state of Yb^{3+} is split into four doublets; T_H^{max} is a characteristic energy of the crystal field splitting between the doublets [22].

In figure 2 we focus on the low-temperature part of the resistivity at high pressures. For $P > 50$ kbar the resistivity shows a sharp change of slope at a temperature T_m well below T_L^{max} . This change of slope is due to the formation of a magnetically ordered state. With increasing pressure T_m is shifted almost linearly to higher temperatures. For the highest pressure $P = 96$ kbar we find $T_m = 1.8$ K. This is still lower than the ordering temperature of the isostructural compound YbNi_2Si_2 which orders magnetically at $T_N = 2.1$ K. The temperature dependence of ρ at $P = 97$ kbar is similar to that of an antiferromagnetically ordered Kondo lattice system like CeCu_2Ge_2 at $P = 0$, e.g. where a magnetic ground state with reduced magnetic moments is formed.

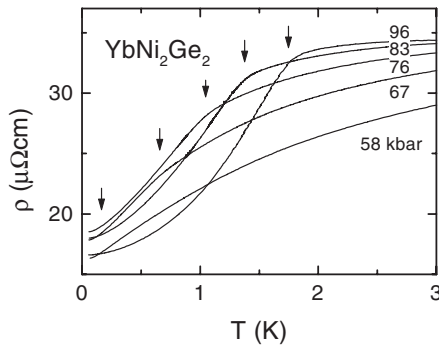


Figure 2. Temperature dependence of the electrical resistivity at low temperatures for various pressures. The arrows indicate the onset of the magnetic order at T_m .

4. Phase diagram and discussion

In figure 3 we summarize the pressure–temperature phase diagram of YbNi_2Ge_2 . It can be well described in a Doniach-type picture [1] due to the competition of the RKKY interaction and the Kondo interaction. At low pressure YbNi_2Ge_2 behaves like an almost intermediate valence system. In the magnetic contribution to the resistivity there is only one maximum at T_H^{max} which is due to Kondo scattering on excited crystal field levels (for T_K larger than the crystal field splitting). At low temperatures a coherent Kondo lattice state is formed below a crossover temperature T_I ; the resistivity follows a T^2 behaviour, which is characteristic of a Fermi liquid ground state (see figure 4).

With increasing pressure T_H^{max} decreases strongly up to $P = 37$ kbar and is constant for

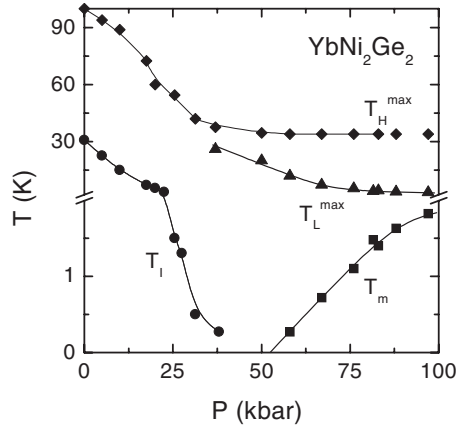


Figure 3. Pressure–temperature phase diagram of YbNi₂Ge₂. T_H^{\max} and T_L^{\max} correspond to the high- and low-temperature maximum of the magnetic contribution of the resistivity. Below T_I a Fermi liquid T^2 temperature dependence is observed in the resistivity. T_m corresponds to the magnetic ordering temperature.

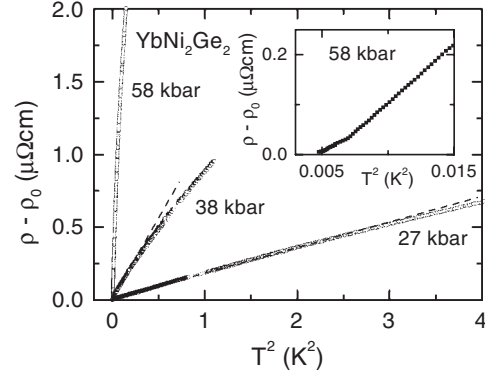


Figure 4. Inelastic scattering contribution $\rho - \rho_0$ as a function of T^2 for different pressures P . The increasing slope reflects the strong increase of the A coefficient. The inset shows the low-temperature behaviour for $P = 58$ kbar in detail, where no T^2 dependence is found for $T \rightarrow 0$.

higher pressures. For $P > 37$ kbar a second maximum at T_L^{\max} develops in the resistivity. The pressure dependence of these two maxima merge at about 30 kbar. From this we expect that, for $P < 30$ kbar, the Kondo temperature is still of the order of the crystal field splitting whereas for higher pressures the Kondo temperature is less than the crystal field splitting. The almost constant T_H^{\max} at high pressures indicates that the crystal field splitting is nearly pressure independent. For $P > 30$ kbar T_L^{\max} represents the energy scale of the Kondo interaction at low temperatures. In the same pressure range T_I also decreases drastically and we can extrapolate that T_I vanishes near 50 kbar, which is close to the critical pressure. In the spin fluctuation theory the decrease of T_I is expected as $T_I = |P - P_c|^{z/2}$, where z is the dynamical critical exponent. For an antiferromagnetic system $z = 2$ and for a ferromagnetic system $z = 3$. Such a pressure dependence of T_I should be observed very close to the QCP. However, in our case the critical point is experimentally not very well defined and we cannot make any final statement, but here the pressure dependence seems to be much stronger than linear.

For $P \gtrsim 50$ kbar YbNi₂Ge₂ has a magnetically ordered ground state. The magnetic transition temperature, determined by the strong change of slope in $\rho(T)$, increases linearly with pressure and reaches $T_m = 1.82$ K for 97 kbar and is expected to increase further with pressure as the isostructural compound YbNi₂Si₂ orders at 2.1 K and the exchange of Si and Ge is mainly a volume effect which influences the hybridization strength in these systems. Spin fluctuation models [7–9] predict a dependence $|P - P_c|^{z/(d+z-2)}$ of T_m in the vicinity of the magnetic instability and $T_m(P)$ is determined by the dynamical critical exponent z and the effective dimensionality d of the spin fluctuation spectrum. A linear pressure dependence is only expected for a quasi-two-dimensional ($d = 2$) magnetic excitation spectrum and is independent of z in this case. However, the magnetic structure and the dimensionality of YbNi₂Ge₂ are unknown up to now, which could manifest this 2D character of the fluctuation spectrum. A linear variation of a magnetic ordering temperature T_m has been found in the CeCu_{6-x}Au_x system [23], where indeed systematic neutron scattering experiments identified the 2D critical fluctuations [24], and in CePd₂Si₂, which is isostructural to YbNi₂Ge₂, near the antiferromagnetic QCP [10, 25, 26]. The tendency to a quasi-two-dimensional character in

CePd₂Si₂ is supported by the magnetic structure with ferromagnetically ordered (110) planes with spins normal to the planes and alternating in the *c* direction [27]. For CeNi₂Ge₂ it has been shown that the magnetic correlations are anisotropic with a quasi-two-dimensional extension in the [110] planes [28]. Furthermore the linear temperature dependence of the resistivity in YbRh₂Si₂ observed over two decades in temperature, the logarithmic increase of the specific heat coefficient $\Delta C/T$ to low temperatures and the strong anisotropy of the susceptibility hint at the possibility of quasi-two-dimensional antiferromagnetic fluctuations coupled to a three-dimensional electronic system [16]. As YbNi₂Si₂ has a helicoidal magnetic structure [21] we expect that the situation in YbNi₂Ge₂ might be more complicated.

In the following we want to focus on the appearance of the magnetic transition. Figure 5 presents the derivative $d\rho/dT$ for different pressures $P > 50$ kbar normalized to the magnetic ordering temperature T_m . At the highest pressure the anomaly of the magnetic transition in the resistivity is sharp and well defined. However, approaching the critical pressure region near 50 kbar, where the magnetic order vanishes, the transition gets less pronounced and the change of the value Δ of $d\rho/dT$ at T_m decreases strongly for $T_m \rightarrow 0$. The same behaviour is found in other systems, like CeIn₃ or CePd₂Si₂, and seems to be a general feature on approaching the magnetically QCP in heavy fermion systems. The decrease in Δ of $(d\rho/dT)$ is shown in the inset of figure 5 as a function of pressure. Δ seems to vanish linearly on approaching the critical pressure. For a mean-field-like transition $d\rho/dT$ is proportional to the specific heat C [29], and we conclude that the observed anomaly in the resistivity corresponds to the size of the anomaly in a specific heat experiment which increases linearly with the ordering temperature T_m too. This is the classical mean field result. In scaling theory the specific heat is expected to have a crossover from a $T_N^{3/2}$ to a linear in T_N behaviour as the QCP is approached from the antiferromagnetic side [30]. Such a crossover to a linear behaviour has been observed experimentally in CePd₂Si₂ and CeIn₃ [26, 31]. The variation of Δ and C as a function of T_m is lower than expected by spin fluctuation theory, where a specific heat

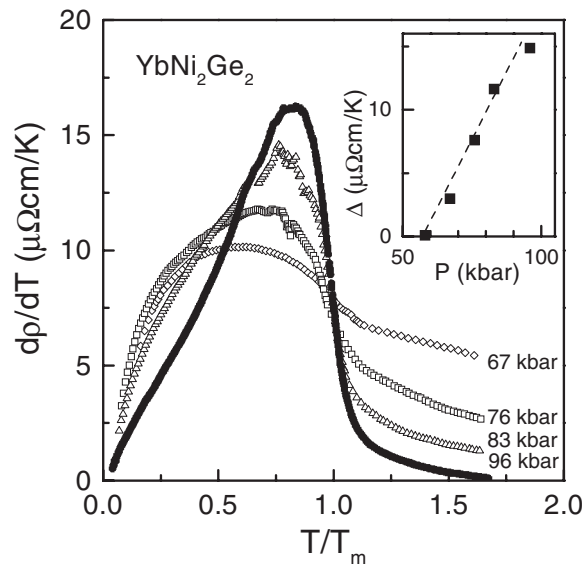


Figure 5. Temperature dependence of the derivative of the resistivity for different pressures P normalized to the transition temperature T_m . The inset shows the value Δ of $d\rho/dT$ at T_m as a function of pressure.

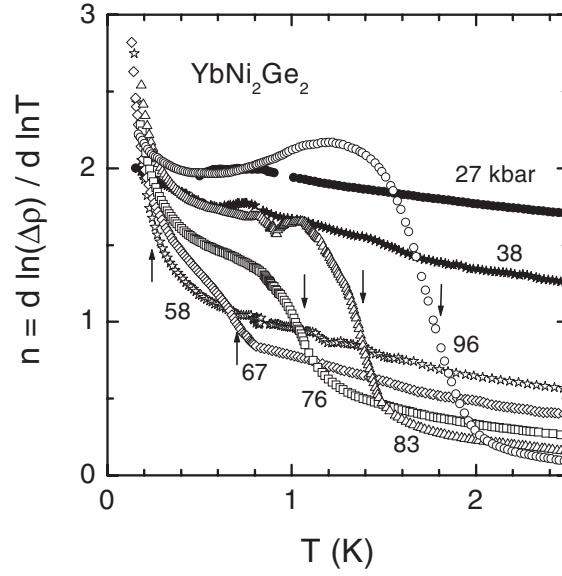


Figure 6. Temperature dependence of the resistivity exponent $n = d \ln(\Delta\rho)/d \ln T$ for different pressures P . The arrows indicate the magnetic ordering at T_m .

jump at the magnetic transition $\Delta C \propto T_m^{(2+z)/z}$ is expected [34]. The linear increase of Δ of $(d\rho/dT)$ with pressure points to an increasing magnetic moment with pressure as Δ of $(d\rho/dT)$ is connected with the sublattice magnetization m . In spin fluctuation theory the pressure dependence of the m can be estimated and $m(P) \propto |P - P_c|^{1/2}$ is expected for both three-dimensional ferromagnetic and antiferromagnetic fluctuations and $m(P) \propto |P - P_c|^{3/4}$ for the two-dimensional antiferromagnetic case [8, 32]. If we assume $\Delta \propto m^2$, which is exact for a weakly ferromagnetic system [33], the observed linear variation of Δ with pressure is in agreement with three-dimensional ferromagnetic and antiferromagnetic fluctuations; however, the linear increase of T_M points to two-dimensional fluctuations. To study the evaluation of $m(P)$ by a direct probe high-pressure ¹⁷⁰Yb Mössbauer spectroscopy experiments are in preparation.

Below we want to discuss the temperature dependence of the resistivity at very low temperatures. Usually the resistivity in a Kondo lattice system can be parametrized at low temperatures in the whole pressure range by a power law dependence $\rho(T) = \rho_0 + A_n T^n$ with an exponent $n = 2$ in the Fermi liquid regime, $n < 2$ close to the QCP and $n > 2$ in the magnetically ordered phase. Figure 6 shows the temperature dependence of the exponent $n = d \ln(\rho - \rho_0)/dT$ for different pressures. At low pressures ($P < 50$ kbar) n increases monotonously and reaches the value $n = 2$ below a finite temperature T_l . However, for $P > 50$ kbar the behaviour changes drastically. We find for every pressure $P > 50$ kbar a strong increase of n at the magnetic ordering temperature T_m and an increasing exponent $n > 2$ for $T < 0.25$ K. The exponent $n > 2$ is characteristic of the additional magnon contribution to the resistivity.

Figure 7 shows the pressure dependence of the A coefficient of the power term of the resistivity. At $P = 0$ the A coefficient of the T^2 term is $A = 7.76$ nΩ cm K⁻². In comparison with the coefficient of the specific heat $\gamma = 130$ mJ mol⁻¹ K⁻² [17] the enhancement of the A coefficient is rather low. In most heavy fermion compounds a ratio

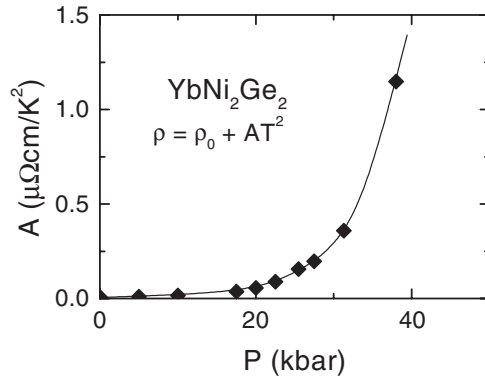


Figure 7. Pressure dependence of the A coefficient of the quadratic term of the resistivity in the paramagnetic regime (the line is drawn to guide the eye).

$A/\gamma^2 \approx 10^{-5} \mu\Omega \text{ cm} (\text{mol K}^2 \text{ mJ}^{-1})^2$ is found [35] and this universal ratio is theoretically confirmed [36, 37]. However, here we find for YbNi_2Ge_2 only a value of $4.6 \times 10^{-7} \mu\Omega \text{ cm} (\text{mol K}^2 \text{ mJ}^{-1})^2$ which is almost two orders of magnitude lower than expected for heavy fermion systems. This low value of A/γ^2 points to an intermediate valence state and can be explained by a conventional band model taking weak many-body correlations into account [40]. The same behaviour is found in other Yb compounds too, e.g. YbAgCu_4 [38, 39] or YbCu_2Si_2 [13]. Furthermore, Kondo hole scattering processes due to imperfections in the Yb sublattice may also influence the temperature dependence of the resistivity for $T \ll T_K$ and an additional term $\rho^{KH} = \rho_0^{KH} - A^{KH}T^2$ has to be considered accounting for the single-ion Kondo scattering at the hole [41]. If such a Kondo hole scattering effect takes place the experimentally observed quadratic coefficient is always reduced by A_{KH} , which leads to the smaller ratio of A/γ^2 .

For $P < 50$ kbar A increases strongly with pressure near 50 kbar. We find $A = 1.15 \mu\Omega \text{ cm K}^{-2}$ for 38 kbar in comparison to $7.76 \text{ n}\Omega \text{ cm K}^{-2}$ at ambient pressure. In figure 8 we plotted the Fermi liquid coefficient A versus T_H^{max} for $P < 40$ kbar on a double-logarithmic scale. The deviations from the slope -2 in this plot indicates the smooth crossover from the intermediate valence with weak correlations to a strongly correlated heavy fermion state due to the change of the ground state degeneracy as observed in CeCu_2Ge_2 around 160 kbar e.g. [44]. Furthermore, on approaching the critical pressure, spin fluctuations become important and the A coefficient is expected to diverge as $|P - P_c|^{-1/2}$ [42, 43]. In YbNi_2Ge_2 the increase of the inelastic magnetic contribution to ρ at the border to the magnetically ordered phase appears even stronger even far from P_c . On the magnetic side of the critical point the A factor is expected to be enhanced too. However, due to the magnetic order, and notably here due to the weak value of T_m , it is difficult to determine the A coefficient of the T^2 term correctly. Close to the magnetic instability the A coefficient takes very large values, as can be seen in the strong slope in figure 4 for $P = 58$ kbar. From this we can estimate $A = 22 \mu\Omega \text{ cm K}^{-2}$. For higher pressures A decreases, indicating the minor influence of spin fluctuation scattering on the resistivity in the magnetic ordered phase.

The pressure dependence of the residual resistivity ρ_0 is shown in figure 9. $\rho_0(P)$ increases monotonously in the paramagnetic regime and has a maximum at $P = 75$ kbar, well inside the magnetically ordered phase. In a real crystal ρ_0 is attributed to various types of imperfections in the lattice, like impurities, missing ions or line defects, is temperature independent and should result only in a very small pressure variation. However, in the presence of electronic correlations these may lead to additional contributions which make the

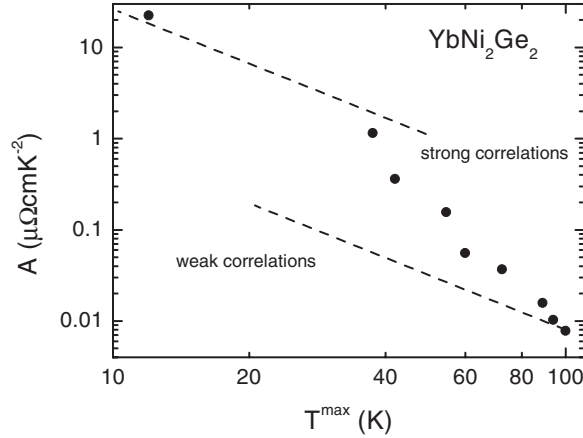


Figure 8. The Fermi liquid coefficient A versus temperature T_H^{\max} (low pressure), or T_L^{\max} ($P = 58$ kbar). The broken line would correspond to $A \propto \gamma^2 \propto (T_H^{\max})^{-2}$. The transition from the weakly to the strongly correlated regime is clear to see.

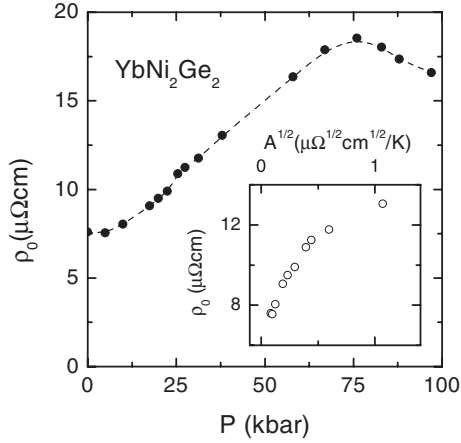


Figure 9. Pressure dependence of the residual resistivity ρ_0 . The inset shows ρ_0 as a function of the square root of the A coefficient.

analysis of $\rho_0(P)$ extremely difficult. In various heavy fermion compounds ρ_0 shows a strong pressure dependence where a maximum is found either in the paramagnetic (e.g. CeCu₂Ge₂, CeCu₂Si₂), at P_c (e.g. MnSi, CeAl₃), or in the magnetically ordered regime (e.g. CeCu₅Au, YbCu₂Si₂) [44–47]. Theoretically it has been suggested that critical fluctuations give rise to an enhancement of the potential scattering of non-magnetic impurity scattering which leads to a sharp cusp structure in the resistivity as a function of pressure near a ferromagnetic QCP. In the case of an antiferromagnet a less pronounced anomaly should be observed [48]. However, no such sharp anomaly is observed in YbNi₂Ge₂ at the critical pressure but a maximum appears well inside the ordered phase like in YbCu₂Si₂. It is argued that only part of the Yb ions orders magnetically at P_c and the maximum of ρ_0 deep in the magnetic phase may coincide with the full ordering at higher pressure [14]. As discussed above, Kondo hole scattering processes lead to a substantial contribution to the residual resistivity ρ_0^{KH} as the perfect lattice periodicity is broken. This Kondo hole scattering is expected to be proportional to m^* . However, from the experimental data it is not possible to separate the Kondo hole contribution from the total residual resistivity $\rho_0(P) = \rho_0^{\text{normal}} + \rho_0^{KH}$. In the inset of figure 9 we plotted $\rho_0(P)$ as a

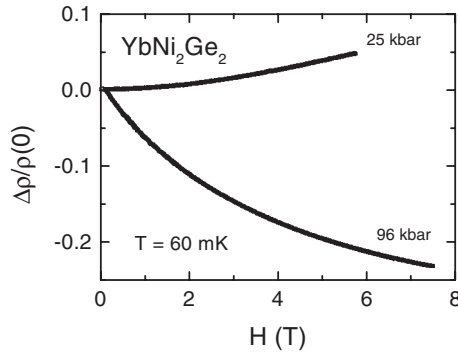


Figure 10. Magnetoresistance $(\rho(H) - \rho(0))/\rho(0)$ for 25 and 96 kbar at $T = 60$ mK for $H \perp (ab)$.

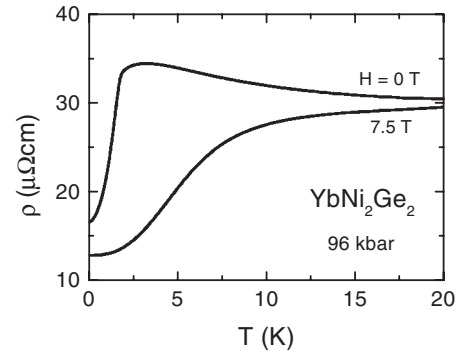


Figure 11. Temperature dependence of the resistivity at 96 kbar for different magnetic fields $H \perp (ab)$.

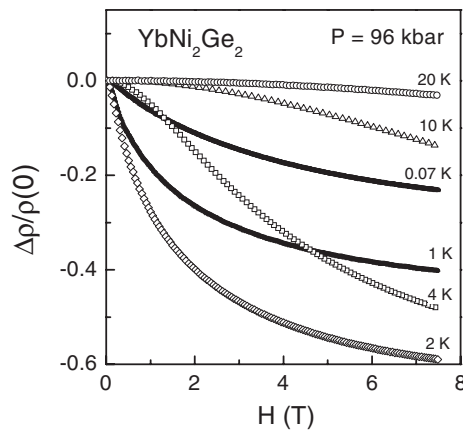


Figure 12. Magnetoresistance $(\rho(H) - \rho(0))/\rho(0)$ at 96 kbar at different temperatures. Full symbols correspond to the magnetically ordered state.

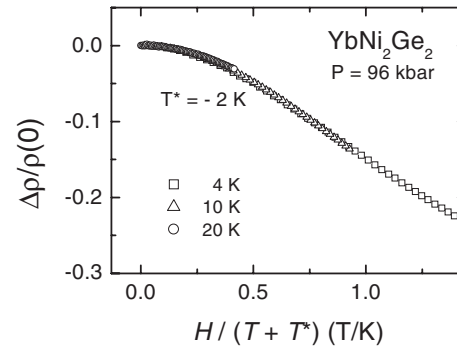


Figure 13. Magnetoresistance $(\rho(H) - \rho(0))/\rho(0)$ versus $H/(T + T^*)$ at 96 kbar for different temperatures $T > T_m$. The analysis gives $T^* = -2$ K.

function of $A^{1/2}$ with pressure as an implicit variable. However, the dependence of ρ_0 on $A^{1/2}$ is lower than linear. That may also indicate the role of charge fluctuation for the Kondo hole.

In the following we discuss the effect of an external magnetic field on the resistivity. Figure 10 shows the magnetoresistance at $T = 60$ mK for $P = 25$ and 96 kbar. At low pressures the magnetoresistance is positive and shows an almost H^2 dependence as expected in the Fermi liquid regime. Up to 5 T the residual resistivity increases by 3.8%. The temperature dependence under an applied magnetic field also shows a T^2 dependence and the A coefficient at 5 T is reduced by 15% and we find $A = 0.125 \mu\Omega \text{ cm K}^{-2}$. As the A coefficient is related to the density of states $N(E_F)$ this corresponds to a decrease of $N(E_F)$ with increasing field as the quasi-particle bands with different spin orientations split in field. In contrast to this the magnetoresistance at high pressure is larger and negative.

Figure 11 shows the temperature dependence of the resistivity at 96 kbar for $H = 0$ and 7.5 T. The very sharp cusp in $\rho(T)$ at T_N gets smoother in field and the maximum due to the incoherent Kondo scattering is suppressed in high magnetic fields as the moments are aligned by the field. In figure 12 we plotted the magnetoresistance at 96 kbar for different temperatures above and below the magnetic ordering at $T_m = 1.8$ K. At temperatures

$T > T_m$, the magnetoresistance can be scaled when plotted as a function of $H/(T + T^*)$ with $T^* = -2$ K (see figure 13). The negative T^* derived in this analysis is clearly inconsistent with an interpretation by a pure Kondo impurity scheme in $H/(T + T^*)$ [49]. Reducing or increasing T^* by 0.2 K makes the scaling significantly worse. Such a scaling has been found in ferromagnetically ordered materials above the ordering temperature, and is theoretically predicted for ferromagnetic spin fluctuation systems [50]. T^* is expected to be equal to the Curie temperature T_c as found here, $T_m \approx -T^*$ in YbNi₂Ge₂. Magnetic susceptibility measurements at ambient pressure do not exclude the ferromagnetic interaction. Below T_m the scaling does not hold anymore, and the field dependence of the magnetoresistance is qualitatively different as additional scattering processes due to the long ranged magnetically ordered state have to be taken in consideration. However, to clarify the nature of the ordered state additional measurements are necessary.

5. Conclusion

We have studied the electrical resistivity of YbNi₂Ge₂ under hydrostatic pressure up to 100 kbar. At low pressures YbNi₂Ge₂ is an almost intermediate valence system and at low temperatures a Fermi liquid state is formed. Increasing pressure leads to a suppression of this state and the A coefficient of the resistivity seems to diverge near a magnetic instability. For $P > 50$ kbar YbNi₂Ge₂ has a magnetically ordered ground state. The magnetic ordering temperature increases almost linearly with pressure. For $P > 50$ kbar the resistivity exponent is significantly higher than 2, indicating the magnon contribution to the resistivity. Interestingly the residual resistivity shows no anomaly at the magnetic instability, but a maximum well inside the magnetically ordered phase. Magnetoresistance measurements at high pressure point out the importance of possibly ferromagnetic interactions. Now that the critical pressure is located near $P_c \approx 50$ kbar, the next step is to fine tune the pressure in hydrostatic conditions.

Acknowledgments

We thank D Jaccard for many fruitful discussions, and K Miyake and J P Sanchez for their critical reading of the manuscript. One of us (GK) acknowledges the ESF within the FERLIN program and the EC (MCFI-1999-00474) for financial support. PCC thanks S L Bud'ko for useful discussions, and N Kelso and N Anderson for assistance in sample preparation. In addition, this work was supported by the Director of Energy Research, Office of Basic Energy Sciences under contract no W-7405-Eng-82.

References

- [1] Doniach S 1977 *Physica B* **91** 231
- [2] Greve N and Steglich F 1991 *Handbook on the Physics and Chemistry of Rare Earth* vol 14 (Amsterdam: Elsevier)
- [3] Jaccard D, Behnia K and Sierro J 1992 *Phys. Lett. A* **163** 475
Jaccard D, Link P, Vargoz E and Alami-Yadri K 1997 *Physica B* **230-2** 297
- [4] Grosche F M, Julian S R, Mathur N D and Lonzarich G G 1996 *Physica B* **223-4** 50
- [5] Movshovich R, Graf T, Mandrus D, Thompson J D, Smith J L and Fisk Z 1996 *Phys. Rev. B* **53** 8241
- [6] Walker I R, Grosche F M, Freye D M and Lonzarich G G 1997 *Physica C* **282-7** 303
- [7] Millis A J 1993 *Phys. Rev. B* **48** 7183
- [8] Moriya T and Takimoto T 1995 *J. Phys. Soc. Japan* **64** 960
- [9] Lonzarich G G 1997 *Electron: A Centenary Volume* ed M Springford (Cambridge: Cambridge University Press) ch 6 p 109

- [10] Mathur N D, Grosche F M, Julian S R, Walker I R, Freye D M, Haselwimmer R K W and Lonzarich G G 1998 *Nature* **394** 39
- [11] Mignot J M and Wittig J 1982 *Valence Instabilities* ed P Wachter and H Boppart (Amsterdam: North-Holland) p 203
- [12] Winkelmann H, Abd-Elmeguid M M, Micklitz H, Sanchez J P, Geibel C and Steglich F 1998 *Phys. Rev. Lett.* **81** 4947
- [13] Alami-Yadri K, Wilhelm H and Jaccard D 1998 *Eur. Phys. J. B* **6** 5
- [14] Winkelmann H, Abd-Elmeguid M M, Micklitz H, Sanchez J P, Vulliet P, Alami-Yadri K and Jaccard D 1999 *Phys. Rev. B* **60** 3324
- [15] Bauer E, Hauser R, Keller L, Fischer P, Trovarelli O, Sereni J G, Rieger J J and Stewart G R 1997 *Phys. Rev. B* **56** 711
- [16] Trovarelli O, Geibel C, Mederle S, Langhammer C, Grosche F M, Gegenwart P, Lang M, Sparn G and Steglich F 2000 *Phys. Rev. Lett.* **85** 626
- [17] Bud'ko S L, Islam Z, Wiener T A, Fisher I R, Lacerda A H and Canfield P C 1999 *J. Magn. Magn. Mater.* **205** 53
- [18] Knebel G, Eggert C, Engelmann D, Viana R, Krimmel A, Dressel M and Loidl A 1996 *Phys. Rev. B* **53** 11 586
- [19] Wilhelm H, Alami-Yadri K, Revaz B and Jaccard D 1999 *Phys. Rev. B* **59** 3651
- [20] Bonville P, Hodges J A, Imbert P, Jéhanno G, Jaccard D and Sierro J 1991 *J. Magn. Magn. Mater.* **97** 178
- [21] André G, Bonville P, Bourée F, Bombik A, Kolenda M, Olés A, Pacyna A, Sikora W and Szytula A 1995 *J. Alloys Comp.* **224** 253
- [22] Cornut B and Coqblin B 1972 *Phys. Rev. B* **5** 4541
- [23] Löhneysen H v 1996 *J. Phys.: Condens. Matter* **8** 9689
- [24] Stockert O, Löhneysen H v, Rosch A, Pyka N and Loewenhaupt M 1998 *Phys. Rev. Lett.* **80** 5627
- [25] Sheikin I, Braithwaite D, Brison J-P, Raymond S, Jaccard D and Flouquet J 2001 *J. Low Temp. Phys.* **122** 591
- [26] Demuer A 2000 *PhD Thesis* University of Grenoble
Demuer A, Jaccard D, Sheikin I, Raymond S, Salce B, Thomasson J, Braithwaite D and Flouquet J 2001 *J. Phys.: Condens. Matter* **13** 9335
- [27] van Dijk N H, Fåk B, Charvolin T, Lejay P and Mignot J M 2000 *Phys. Rev. B* **61** 8922
- [28] Fåk B, Flouquet J, Lapertot G, Fukuhara T, and Kadowaki H 2000 *J. Phys.: Condens. Matter* **12** 5423
- [29] Alexander S, Helman J S and Balberg I 1976 *Phys. Rev. B* **13** 304
- [30] Continentino M A 2001 *Quantum Scaling in Many-Body Physics* (Singapore: World Scientific)
- [31] Knebel G, Braithwaite D, Canfield P, Lapertot G and Flouquet J 2002 *Phys. Rev. B* at press
- [32] Moriya T and Ueda K 2000 *Adv. Phys.* **49** 555
- [33] Moriya T 1979 *J. Magn. Magn. Mater.* **14** 1
- [34] Zülicke U and Millis A J 1995 *Phys. Rev. B* **51** 8996
- [35] Kadowaki K and Woods S B 1986 *Solid State Commun.* **58** 507
- [36] Takimoto T and Moriya M 1996 *Solid State Commun.* **99** 457
- [37] Continentino M A 2000 *Eur. Phys. J. B* **13** 31
- [38] Bauer E, Hauser R, Gratz E, Payer K, Oomi G, and Kagayama T 1993 *Phys. Rev. B* **48** 15 873
- [39] Graf T, Movshovich R, Thompson J D, Fisk Z and Canfield P C 1995 *Phys. Rev. B* **52** 3099
- [40] Miyake K, Matsuura T and Varma C M 1989 *Solid State Commun.* **71** 1149
- [41] Lawrence J M, Thompson J D and Chen Y Y 1985 *Phys. Rev. Lett.* **54** 2537
- [42] Ueda K and Moriya T 1975 *J. Phys. Soc. Japan* **39** 605
- [43] Ueda K 1977 *J. Phys. Soc. Japan* **43** 1497
- [44] Jaccard D, Wilhelm H, Alami-Yadri K and Vargoz E 1999 *Physica B* **259–61** 1
- [45] Thessieu C, Flouquet J, Lapertot G, Stepanov A N and Jaccard D 1995 *Solid State Commun.* **95** 707
- [46] Jaccard D and Sierro J 1995 *Physica B* **206–7** 625
- [47] Wilhelm H, Raymond S, Jaccard D, Stockert O, Löhneysen H v and Rosch A 2001 *J. Phys.: Condens. Matter* **13** L329
- [48] Miyake K and Maebashi H 2001 *J. Phys. Chem. Solids* **62** 53
Miyake K and Narikiyo O unpublished
- [49] Schlottmann P 1983 *Z. Phys. B* **51** 223
- [50] Yamada H and Takada S 1972 *Prog. Theor. Phys.* **48** 1828